




Investigation of Hall current and thermal diffusion effects on unsteady MHD mixed convective Jeffrey fluid flow over an inclined permeable surface with chemical reaction

N. Kanimozhi¹, R. Vijayaragavan^{1,a}, B. Rushi Kumar^{2,b} , Ali J. Chamkha³

¹ Department of Mathematics, Thiruvalluvar University, Serkkadu, Vellore, Tamil Nadu 632115, India

² Department of Mathematics, School of Advanced Sciences, Vellore Institute of Technology, Vellore, Tamil Nadu 632014, India

³ Faculty of Engineering, Kuwait College of Science and Technology, Doha, Kuwait

Received: 15 January 2024 / Accepted: 7 March 2024

© The Author(s), under exclusive licence to Società Italiana di Fisica and Springer-Verlag GmbH Germany, part of Springer Nature 2024

Abstract Jeffrey fluids, a subset of non-Newtonian fluids, have received substantial research attention owing to their versatile utility in industries, such as polymer processing, cosmetics, and glass manufacturing. This paper endeavors to introduce a pioneering outlook on the behavior of Jeffrey fluids by researching their intricate responses to an array of influencing factors, including slip conditions, thermal effects, magnetic fields, chemical influences, and pivotal roles in the enhancement of drug delivery systems. Jeffrey fluids hold particular significance in modeling physiological fluids found in biological systems, representing blood circulation with precision in terms of relaxation time and stress retardation. Interestingly, under specific conditions, when subjected to wall shear stress exceeding the yield strength, Jeffrey fluids transition to exhibit Newtonian fluid characteristics. Hence, we embark on a comprehensive exploration of the applicability of the Jeffrey fluid model across diverse industrial domains and its contribution to the realm of flow control. Our research focuses on the study of mixed convective Jeffrey fluid flow across an inclined vertical plate, considering the combined impacts of the Soret and Hall currents, along with slip conditions involving velocity, temperature, and concentration disparities. This intricate problem is analytically resolved through the careful use of the perturbation technique. Furthermore, the inclined angle parameter enhances the velocity profile, while the velocity slip parameter exhibits the opposite effect. Additionally, the thermal and concentration slip parameters attenuate the temperature and concentration profiles.

Abbreviations

g	Acceleration due to gravity (m/s^2)
α	Angle of inclined parameter ($^\circ$)
γ	Aligned magnetic field
T^*	Fluid temperature (K)
T_∞^*	Ambient temperature (K)
C^*	Concentration of the fluid (mol m^{-3})
C_∞^*	Ambient concentration (mol m^{-3})
σ	Electrical conductivity (S m^{-1})
B_0	Applied magnetic field
ρ	Density of the fluid (Kg/m^3)
ν	Kinematic viscosity ($\text{m}^2 \text{s}^{-1}$)
m	Hall current parameter
k	Thermal conductivity (W/mK)
C_p	Specific heat at constant pressure (J/Kg K)
λ	Jeffrey fluid parameter
K^*	Permeability of the porous medium (m^2)
K_p	Permeability of the porous parameter (m^2)
D_m	Molecular diffusivity ($\text{m}^2 \text{s}^{-1}$)
R	Radiation parameter
Pr	Prandtl number

^a e-mail: rvijayaraagavantvu@gmail.com

^b e-mail: rushikumar@vit.ac.in (corresponding author)

M	Magnetic field parameter
Q	Heat generation/absorption parameter (J/K)
Kr	Chemical reaction parameter (S^{-1})
Sr	Soret number
Gr	Thermal Grashof number
Gm	Mass Grashof number
h_1	Velocity slip parameter
h_2	Thermal slip parameter
h_3	Concentration slip parameter

1 Introduction

Non-Newtonian fluids have attracted considerable interest among researchers due to their exceptional versatility in various industrial domains, ranging from polymer processing to cosmetics and glass manufacturing. Notably, Jeffrey fluids, a specific type of non-Newtonian fluid, exhibit properties that make them ideal for modeling, physiological fluids in biological systems, such as blood circulation. These fluids aptly describe relaxation time and stress retardation, offering valuable insights into complex biological processes. Additionally, Jeffrey fluids demonstrate unique behavior resembling a hybrid of a liquid and a solid, making them essential for characterizing polymer solutions and certain biological fluids. The ability to comprehend the dynamics of Jeffrey fluids and their interactions with heat, chemical, and magnetic fields holds immense potential for developing precise and efficient drug delivery systems, thereby revolutionizing medical treatment methodologies. Furthermore, the application of the Jeffrey fluid model extends beyond the realm of biology, finding utility in industries involving foams, syrups, polymeric and metallurgical materials, and flow control.

Electrically conductive fluids interacting with magnetic fields have numerous applications, including nuclear reactors, geothermal energy, oil exploration, and hypersonic flight. The field of magnetohydrodynamics (MHD), introduced by Alfven [1], has become essential for thermal insulation, plastic film extrusion, submarines, nuclear reactors, power generation, and oil reservoirs. MHD flows through porous media have garnered the interest of scholars owing to their practical implications in agriculture for irrigation, groundwater resources, purification processes, filtration, oil extraction, etc. Several research studies have investigated the behavior of unsteady Jeffrey fluid flowing through porous media with different geometries. Manjunatha et al. [2] studied the effects of variable transport properties and slip on MHD Jeffrey fluid flow through channels. HariBabu et al. [3] obtained a Laplace transform solution for an unsteady MHD rotating Jeffrey fluid over a vertically moving porous plate.

Hall currents are components of electric currents that flow at right angles to magnetic and electrical induction forces. Pioneering work on Hall currents was performed by Hall [4]. Fiza et al. [5] assessed the effect of the Hall current between two parallel plates on the rotating flow of MHD Jeffrey fluid. Ullah et al. [6] discussed the Hall current in the Jeffrey nanofluid flow on a rotating frame. Krishna [7] described how Hall and ion effects can cause unsteady MHD Jeffrey fluid flow across an infinite vertically permeable plate with increasing wall temperature. Raju et al. [8] studied the free convective Casson fluid flow past a vertically inclined plate submitted to a magnetic field in the presence of heat and mass transfer. However, radiation plays a key role in many engineering fields, including fossil fuel combustion, gas turbines, solar energy, and astrophysical fluxes that occur at high temperatures. Raju et al. [9] examined the unsteady MHD mixed convection of a Jeffrey fluid with thermal radiation. Manjula et al. [10] analyzed the impact of the Hall current and radiation on an inclined vertical plate. Kanimozhi et al. [11] discussed the effects of radiation on a second-stage fluid. Qasim [12] analyzed the heat source/sink for heat and mass transfer in a Jeffrey fluid through a stretch film. Hayat et al. [13] analyzed the radiative flow of a Jeffrey fluid with a heat source. Peristaltic fluid transport occurs in an extensible tube as a contraction/expansion wave propagates. It has many physiological applications, such as the movement of food through the digestive system, the migration of digestate in the gastrointestinal tract, and the flow of blood in blood vessels. Several research studies [14–17] have been conducted to examine the characteristics of peristaltic flow in Jeffrey fluid.

The presence of a no-slip boundary condition is observed when the fluid particles are in close proximity to the surface and are unable to move in conjunction with it or when adhesion prevails over cohesion. Viscous fluids are an exception to this phenomenon because when walls are smooth enough, a solid surface can cause them to slip. Slip conditions become important in many situations, such as for wire mesh, lubricated surfaces, and rough and coated surfaces. In addition, heat and mass transport, along with chemical reactions, have been greatly amplified owing to the variety of uses inherent in nature and current technology. Chemical processes that occur in fluid flow include ceramic manufacturing, refrigeration, mist generation, and cooling towers. The Soret effect refers to the mass flow caused by a temperature gradient. Many authors have incorporated the Soret effect into their research to address these problems because of its importance. Babu et al. [18] examined the unsteady MHD-free convective flow of a viscoelastic fluid past an infinite vertical porous moving plate with variable temperature and concentration. Sk et al. [19] analyzed multiple slip effects on the bio convection of nanofluid flows containing gyrotactic microorganisms and nanoparticles. Kanimozhi et al. [20] discussed multiple slip impacts on an unsteady MHD micropolar fluid over a stretched foil. Balamurugan et al. [21] illustrated unsteady MHD flow with a chemical reaction. SatyaNarayana et al. [22] described a numerical approach to studying the consequences of chemical processes and heat sources on a Jeffrey fluid passing over a stretching layer. Das et al. [23] investigated the radiative flow of MHD

Jeffrey fluid past a stretching sheet with surface slip and melting heat transfer. Kumar et al. [24] studied a finite element technique for a Jeffrey fluid with Soret number effects. Gulle et al. [25] explained the chemical process and the Soret effect on MHD Jeffrey flow over an inclined vertical plate implanted in a porous medium. Kumar et al. [26] investigated the effects of a Soret, a Dufour, a Hall current and rotation on MHD natural convective heat and mass transfer flow past an accelerated vertical plate through a porous medium. Nisar et al. [27] used the Adomian decomposition (ADM) method to determine the MHD of a Jeffrey fluid under a heat source and chemical process.

Many practical applications involve fluid flow over inclined surfaces or through porous media. Investigating the flow of Jeffrey fluids over inclined surfaces or through porous media provides valuable insights into the behavior of these fluids in realistic scenarios and helps optimize the design and operation of relevant engineering systems. With respect to the unsteady MHD convective flow of a Jeffrey fluid, various studies [28–37] have contributed to the fundamental understanding of fluid dynamics and provided insights into complex flow phenomena. The recent surge in research on magnetohydrodynamic (MHD) flows involving Jeffrey fluids has produced valuable insights into their intricate behaviors. This literature review synthesizes findings from several key studies, offering a comprehensive overview of the advancements made in this field.

Ibrahim and Abou-zeid [38] initiated this exploration by employing computational simulation techniques to investigate the peristaltic transport of Jeffrey fluid via density-dependent parameters in MHDs. Their work laid the foundation for subsequent studies, providing a computational framework for understanding the complex interactions in such fluid systems. Building upon this foundation, Dong et al. [39] investigated the electromagnetic electroosmotic flow of Jeffrey fluid through a semicircular microchannel. Their research shed light on the unique electrokinetic phenomena within microchannels, offering practical implications for engineering applications. Thenmozhi et al. [40] extended the investigation to MHD flows with stretching porous sheets in a heat transfer system involving Jeffrey fluid. Their analysis contributed to the understanding of heat transfer dynamics in these systems, adding a layer of complexity to the existing body of knowledge. Li et al. [41] explored the pulse electromagnetic flow of Jeffrey fluid in parallel plate microchannels, emphasizing the dynamic response of the fluid to pulsatile electromagnetic fields. This study provides valuable insights into potential applications in microfluidic devices and further expands the scope of related research. In a more recent contribution, Khan et al. [42] conducted a thermal examination of double diffusive MHD Jeffrey fluid flow through the space of the disk and cone apparatus subject to multiple rotations. This work added a novel dimension by considering the impact of rotational forces, broadening the understanding of complex fluid behaviors in diverse geometries.

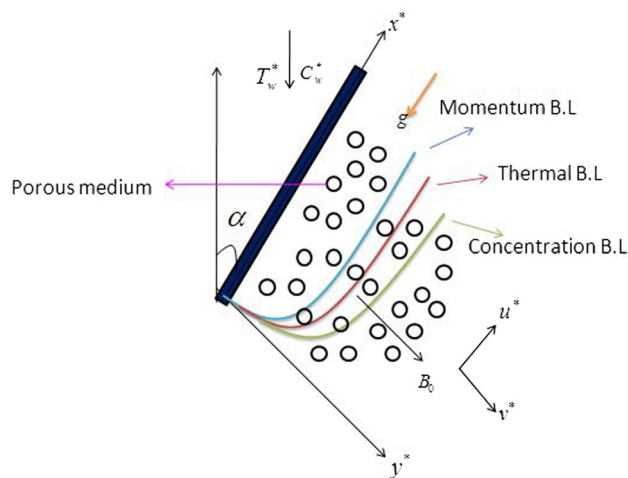
In conclusion, these studies collectively contribute to the evolving landscape of magnetohydrodynamic flows involving Jeffrey fluids. From computational simulations to practical applications in microfluidics and heat transfer systems, the research highlighted in this literature review underscores the importance of continued exploration of this intriguing intersection of fluid dynamics and electromagnetism. While previous studies have focused primarily on Jeffrey fluid flow across an inclined vertical plate under the assumption of no-slip conditions, investigations into velocity boundary conditions under slip conditions are limited. A comprehensive exploration of slip regimes across all boundary conditions has yet to be performed. This study aims to bridge this research gap by considering a mixed convective Jeffrey fluid flowing over an inclined vertical plate, wherein the influences of the Soret and Hall currents, as well as slip conditions encompassing velocity slip, temperature jumps, and concentration jumps, are incorporated. The problem is approached analytically by employing the perturbation technique to provide a deeper understanding of the behavior exhibited by Jeffrey fluids in complex flow scenarios.

2 Mathematical modeling

An unsteady 2D MHD mixed convective flow of a viscous fluid conducting electricity in an inclined vertical plate saturated with a porous media and a Hall current is considered. Consider the Cartesian system x^* as an axis along the plate and an y^* axis that is perpendicular to it. Since the plate has an infinite length, the physical quantities will be independent of the x^* direction. Let u^* and v^* be the velocity components along the x^* and y^* axes, respectively. In the fluid medium, the origin is stationary, with an ambient temperature T_∞ , while the plate maintains a uniform temperature T_w . The plate concentration remains uniform at C_w , while the concentration of the ambient fluid is represented by C_∞ . A uniform transverse magnetic field force B_0 is applied perpendicular to the direction of flow. The following assumptions are made for our study.

- i. The induced magnetic field is negligibly small compared to the applied magnetic field due to the lower magnetic Reynolds number.
- ii. Viscous dissipation and ohmic heating are disregarded in this scenario due to the low velocity and viscosity of the fluid flow. This omission is justified by the negligible impact these factors have on the overall dynamics, given the subdued flow conditions.
- iii. The consideration of slip conditions is crucial in diverse scenarios, encompassing wire mesh, lubricated surfaces, and coated surfaces. Consequently, they are carefully factored into the analysis to ensure an accurate representation of the system's behavior.
- iv. The analysis accounts for the concentration dynamics of the species involved in a first-order chemical reaction. Additionally, it incorporates the Soret effect, which arises due to temperature gradients. By integrating these factors, this investigation aims to provide a comprehensive understanding of how chemical reactions and thermal variations interact within a system.

Fig. 1 Flow geometry of the problem



Following the above assumptions, we can formulate the conservation of momentum, energy and concentration that govern the mixed convective boundary layer flow over an inclined vertical plate immersed in a porous medium with a slip regime as follows (Fig. 1).

The continuity, momentum, and energy equations are [25]

$$\frac{\partial v^*}{\partial y^*} = 0 \tag{1}$$

$$\begin{aligned} \frac{\partial u^*}{\partial t^*} + v^* \left(\frac{\partial u^*}{\partial x^*} + \frac{\partial u^*}{\partial y^*} \right) = & -\frac{1}{\rho} \frac{\partial p^*}{\partial x^*} + \left(\frac{v}{1+\lambda} \right) \left(\frac{\partial^2 u^*}{\partial x^{*2}} + \frac{\partial^2 u^*}{\partial y^{*2}} \right) + g\beta(T^* - T_\infty) \cos \alpha \\ & + g\beta^*(C^* - C_\infty) \cos \alpha - \frac{\sigma B_0^2}{\rho(1+m^2)} \sin^2 \gamma u^* - \frac{vu^*}{K^*} \end{aligned} \tag{2}$$

$$\frac{\partial T^*}{\partial t^*} + v^* \left(\frac{\partial T^*}{\partial x^*} + \frac{\partial T^*}{\partial y^*} \right) = \frac{k}{\rho C_p} \left(\frac{\partial^2 T^*}{\partial x^{*2}} + \frac{\partial^2 T^*}{\partial y^{*2}} \right) - \frac{1}{\rho C_p} \frac{\partial q_r^*}{\partial y^*} - \frac{Q^*}{\rho C_p} (T^* - T_\infty) \tag{3}$$

$$\frac{\partial C^*}{\partial t^*} + v^* \left(\frac{\partial C^*}{\partial x^*} + \frac{\partial C^*}{\partial y^*} \right) = D_m \left(\frac{\partial^2 C^*}{\partial x^{*2}} + \frac{\partial^2 C^*}{\partial y^{*2}} \right) - \text{Kr}^*(C^* - C_\infty) + \frac{D_M K_T}{T_M} \left(\frac{\partial^2 T^*}{\partial x^{*2}} + \frac{\partial^2 T^*}{\partial y^{*2}} \right) \tag{4}$$

The boundary conditions with slip are given by [21]

$$u^* = u_w^* + h_1^* \frac{\partial u^*}{\partial y^*}, T^* = T_w^* + h_2^* \frac{\partial T^*}{\partial y^*}, C^* = C_w^* + h_3^* \frac{\partial C^*}{\partial y^*} \text{ at } y^* = 0 \tag{5}$$

$$u^* \rightarrow U_\infty^* = U_0(1 + \varepsilon e^{n^* t^*}), T^* \rightarrow T_\infty^*, \text{ and } C^* \rightarrow C_\infty^* y^* \rightarrow \infty \tag{6}$$

Here, the plate depends on the time-varying suction and can be expressed as

$$v^* = -V_0(1 + \varepsilon A e^{n^* t^*}) \tag{7}$$

where A is a real positive constant, ($\varepsilon, \varepsilon A < 1$), and V_0 is a suction velocity parameter.

Equation (2) gives the following results outside the boundary layer:

$$-\frac{1}{\rho} \frac{\partial p^*}{\partial x^*} = \frac{\partial U_\infty^*}{\partial t^*} + \frac{v}{K^*} U_\infty^* + \frac{\sigma B_0^2}{\rho(1+m^2)} U_\infty^* \sin^2 \gamma \tag{8}$$

Let us consider a gray gas equilibrium that is optically thin in the form q_r^* :

$$\frac{\partial q_r^*}{\partial y^*} = 4(T^* - T_\infty)I' \tag{9}$$

Now, let us describe the nondimensional parameters

$$\left. \begin{aligned} u &= \frac{u^*}{U_0}, t = \frac{t^* V_0^2}{4v}, y = \frac{V_0 y^*}{v}, U_\infty = \frac{U_\infty^*}{U_0}, u_w = \frac{u_w^*}{U_0} \\ \theta &= \frac{T^* - T_\infty^*}{T_w^* - T_\infty^*}, \phi = \frac{C^* - C_\infty^*}{C_w^* - C_\infty^*}, K_p = \frac{v K^*}{V_0^2}, n = \frac{4vn^*}{V_0^2}, R = \frac{4I'v}{\rho C_p V_0^2} \\ Gr &= \frac{vg\beta(T_w^* - T_\infty^*)}{U_0 V_0^2}, Gm = \frac{vg\beta^*(C_w^* - C_\infty^*)}{U_0 V_0^2}, Pr = \frac{\mu C_p}{k}, \\ M &= \frac{\sigma B_0^2 v}{\rho V_0^2}, Q = \frac{Q^* v}{V_0^2}, Sc = \frac{v}{D_m}, Kr = \frac{Kr^* v}{V_0^2}, Sr = \frac{D_M K_T (T_w^* - T_\infty^*)}{T_M (C_w^* - C_\infty^*)} \end{aligned} \right\} \tag{10}$$

The governing equations are reduced to a dimensionless form as follows:

$$\frac{1}{4} \frac{\partial u}{\partial t} - (1 + \varepsilon A e^{nt}) \frac{\partial u}{\partial y} = \frac{1}{4} \frac{dU_\infty}{dt} + \lambda_1 \frac{\partial^2 u}{\partial y^2} + N(U_\infty - u) + Gr\theta \cos \alpha + Gm\phi \cos \alpha \tag{11}$$

$$\frac{1}{4} \frac{\partial \theta}{\partial t} - (1 + \varepsilon A e^{nt}) \frac{\partial \theta}{\partial y} = \frac{1}{Pr} \frac{\partial^2 \theta}{\partial y^2} - \xi \theta \tag{12}$$

$$\frac{1}{4} \frac{\partial \phi}{\partial t} - (1 + \varepsilon A e^{nt}) \frac{\partial \phi}{\partial y} = \frac{1}{Sc} \frac{\partial^2 \phi}{\partial y^2} - Kr\phi + Sr \frac{\partial^2 \theta}{\partial y^2} \tag{13}$$

where $M_1 = \frac{M^2}{1+m^2}$, $N = (M_1 \sin^2 \gamma + 1/K_p)$, $\lambda_1 = (\frac{1}{1+\lambda})$, $\xi = R + Q$.

The associated boundary conditions become

$$u = u_w + h_1 \frac{\partial u}{\partial y}, \theta = 1 + h_2 \frac{\partial \theta}{\partial y}, \phi = 1 + h_3 \frac{\partial \phi}{\partial y}, \text{ at } y = 0 \tag{14}$$

$$u \rightarrow 0, \theta \rightarrow 0, \phi \rightarrow 0 \text{ as } y \rightarrow \infty \tag{15}$$

2.1 Method of solution

To investigate the behavior of a mixed convective Jeffrey fluid over an inclined vertical plate, we utilize the perturbation technique for solving analytic problems. This approach allows us to derive insightful results and unravel the intricate dynamics of the fluid. By employing this methodology, we aim to provide valuable insights into the behavior of Jeffrey fluids, shedding light on their unique characteristics and potential applications. PDEs (11)–(13) were not solvable in closed form. Therefore, these equations turn into ordinary differential equations (ODEs) with the perturbation technique. We assumed the following substitutions for the velocity field, temperature field, and concentration field.

$$u = u_0(y) + \varepsilon u_1(y)e^{nt} + O(\varepsilon^2) \tag{16}$$

$$\theta = \theta_0(y) + \varepsilon \theta_1(y)e^{nt} + O(\varepsilon^2) \tag{17}$$

$$\phi = \phi_0(y) + \varepsilon \phi_1(y)e^{nt} + O(\varepsilon^2) \tag{18}$$

We can obtain the following equation by substituting Eqs. (16) to (18) into Eqs. (11) to (13) and equating the zeroth- and first-order terms without including the higher-order terms.

$$\lambda_1 u_0''(y) + u_0'(y) - Nu_0(y) = -Gr\theta_0(y) \cos \alpha - Gm\phi_0(y) \cos \alpha - N \tag{19}$$

$$\theta_0''(y) + Pr \theta_0'(y) - Pr \xi \theta_0(y) = 0 \tag{20}$$

$$\phi_0''(y) + Sc\phi_0'(y) - ScKr\phi_0(y) = -ScSr\theta_0''(y) \tag{21}$$

$$\begin{aligned} \lambda_1 u_1''(y) + u_1'(y) - \left(N + \frac{n}{4}\right)u_1(y) &= -Gr\theta_1(y) \cos \alpha - Gm\phi_1(y) \cos \alpha \\ &\quad - \left(N + \frac{n}{4}\right) - Au_0'(y) \end{aligned} \tag{22}$$

$$\theta_1''(y) + Pr \theta_1'(y) - Pr \left(\xi + \frac{n}{4}\right)\theta_1(y) = -Pr A\theta_0'(y) \tag{23}$$

$$\phi_1''(y) + Sc\phi_1'(y) - Sc \left(Kr + \frac{n}{4}\right)\phi_1(y) = -ScA\phi_0'(y) - ScSr\theta_1''(y) \tag{24}$$

With the corresponding boundary conditions

$$u_0 = u_w + h_1 \frac{\partial u_0}{\partial y}, u_1 = h_1 \frac{\partial u_1}{\partial y}, \theta_0 = 1 + h_2 \frac{\partial \theta_0}{\partial y}, \theta_1 = h_2 \frac{\partial \theta_1}{\partial y}, \tag{25}$$

$$\begin{aligned} \phi &= 1 + h_3 \frac{\partial \phi_0}{\partial y}, \phi_1 = h_3 \frac{\partial \phi_1}{\partial y} \text{ at } y = 0 \\ u_0 \rightarrow 1, u_1 \rightarrow 1, \theta_0 \rightarrow 0, \theta_1 \rightarrow 0, \phi_0 \rightarrow 0, \phi_1 \rightarrow 0 \text{ as } y \rightarrow \infty \end{aligned} \tag{26}$$

By applying boundary conditions (25) and (26) to solve Eqs. (19) - (24), we obtain

$$u_0 = A_{10}e^{-m_5y} + A_{11}e^{-m_3y} + A_{12}e^{-m_1y} + 1 \tag{27}$$

$$u_1 = A_{13}e^{-m_6y} + A_{14}e^{-m_5y} + A_{15}e^{-m_4y} + A_{16}e^{-m_3y} + A_{17}e^{-m_2y} + A_{18}e^{-m_1y} + 1 \tag{28}$$

$$\theta_0 = A_1e^{-m_1y} \tag{29}$$

$$\theta_1 = A_2e^{-m_2y} + A_3e^{-m_1y} \tag{30}$$

$$\phi_0 = A_4e^{-m_3y} + A_5e^{-m_1y} \tag{31}$$

$$\phi_1 = A_6e^{-m_4y} + A_7e^{-m_3y} + A_8e^{-m_2y} + A_9e^{-m_1y} \tag{32}$$

Equations (27)–(32) can be written in the form of (16)–(18):

$$\begin{aligned} u &= A_{10}e^{-m_5y} + A_{11}e^{-m_3y} + A_{12}e^{-m_1y} + 1 \\ &+ \varepsilon e^{nt} (A_{13}e^{-m_6y} + A_{14}e^{-m_5y} + A_{15}e^{-m_4y} + A_{16}e^{-m_3y} + A_{17}e^{-m_2y} + A_{18}e^{-m_1y} + 1) \end{aligned} \tag{33}$$

$$\theta = A_1e^{-m_1y} + \varepsilon e^{nt} (A_2e^{-m_2y} + A_3e^{-m_1y}) \tag{34}$$

$$\phi = A_4e^{-m_3y} + A_5e^{-m_1y} + \varepsilon e^{nt} (A_6e^{-m_4y} + A_7e^{-m_3y} + A_8e^{-m_2y} + A_9e^{-m_1y}) \tag{35}$$

2.2 Skin friction coefficient

$$\begin{aligned} \tau &= \left(\frac{\partial u}{\partial y} \right)_{y=0} \\ &= -(m_5A_{10} + m_3A_{11} + m_1A_{12}) - \varepsilon e^{nt} (m_6A_{13} + m_5A_{14} + m_4A_{15} + m_3A_{16} + m_2A_{17} + m_1A_{18}) \end{aligned} \tag{36}$$

2.3 Nusselt number

$$\begin{aligned} \text{Nu} &= -\left(\frac{\partial \theta}{\partial y} \right)_{y=0} \\ &= m_1A_1 + \varepsilon e^{nt} (m_2A_2 + m_1A_3) \end{aligned} \tag{37}$$

2.4 Sherwood number

$$\begin{aligned} \text{Sh} &= -\left(\frac{\partial \phi}{\partial y} \right)_{y=0} \\ &= m_3A_4 + m_1A_5 + \varepsilon e^{nt} (m_4A_6 + m_3A_7 + m_2A_8 + m_1A_9) \end{aligned} \tag{38}$$

3 Results and discussion

The dynamics of unsteady mixed convective Jeffrey fluid flow around an inclined vertical plate in a porous medium in the presence of a slip flow regime are explored in this paper. In particular, the effects of hall current, heat generation, thermal radiation, and the Soret effect are closely examined. To provide important insights into the theoretical and practical aspects of fluid dynamics in porous media under MHD effects, this study attempts to fully comprehend the complex interactions and behaviors of intricate systems. By applying perturbation techniques, researchers can effectively address these intricate equations and derive analytical solutions, providing valuable insights. The values of the relevant parameters are taken as $\varepsilon = 0.001$, $Gm = 3$, $K_p = 0.5$, $Kr = 1$, $R = 0.5$, $A = 1$, $Sr = 0.5$, $h_1 = 0.4$, $h_2 = 0.5$, $h_3 = 1$ and from a previous study [25]. Figure 2 shows the velocity profiles for various magnetic field parameters M . As M increases, the velocity decreases since the Lorentz force acts against the current. That is, when charged particles or fluids move within a magnetic field, they effectively function as a resistance force, preventing their motion. Therefore, the Lorentz force increases as the magnetic field parameter increases, which cause the velocity to decrease. As the dimensionless parameter for porous media increases, the velocity also increases. This outcome is expected if we disregard

Fig. 2 Velocity profiles for different values of M

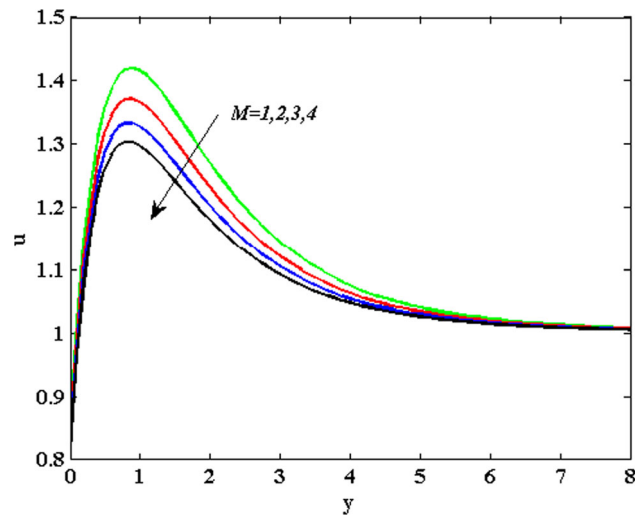
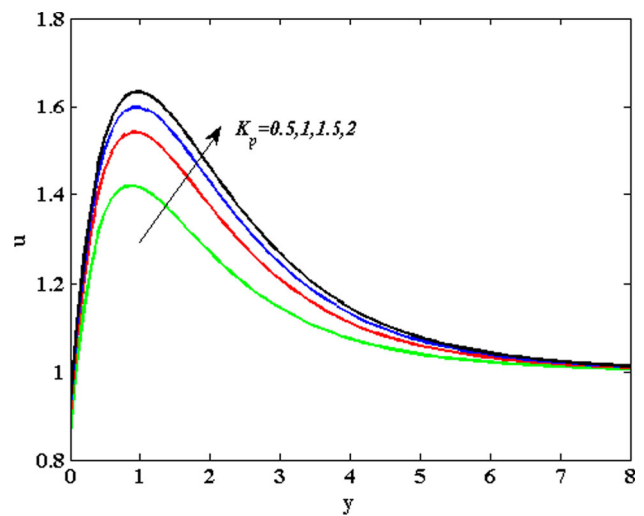


Fig. 3 Velocity profiles for different values of K_p



the permeability of the porous medium from a physical standpoint. The permeability of the porous parameter K_p influences the velocity profile in Fig. 3, which increases with increasing permeability of the porous medium. When the dimensionless porous media parameter increases, the velocity also increases. Physically, if the permeability of a porous medium is ignored, this result is likely. Figure 4 shows the velocity profile for various Hall current parameters m . The velocity profile increases when m boosts because the fluid's increased electrical conductivity promote molecular mobility, which enhances the fluid's velocity. This is a result of the resistive damping effect of the applied magnetic field. It is clear from this relationship how magnetic fields affect particle motion or fluid dynamics, especially when a Hall current is present. The velocity profiles for thermal Grashof number Gr and mass Grashof number Gm are shown in Figs. 5 and 6, respectively. The Grashof number illustrates the interaction between buoyant and viscous forces within a fluid layer. As Gr increases, the thermal buoyancy force becomes more dominant than the viscous force, leading to a decrease in the flow resistance. This results in a sharp increase in fluid velocity near the wall, followed by a gradual decrease toward zero in a uniform manner. Thus, the maximum peak velocity occurs when Gr and Gm increases. Figure 7 shows the velocity profile for the Jeffrey fluid parameter λ . As λ increases, the velocity decreases. It safeguards the inherent physical properties of the fluid. Figure 8 shows the velocity profile for inclined angle parameter α . According to the statistics, the velocity profile decreases as α increases. The velocity profile for the velocity slip parameter h_1 is given in Fig. 9, which increases as h_1 increases. This phenomenon is due to the reduced friction between the fluid and the plate, allowing for greater flow near the surface. As a result, the velocity gradient near the wall decreases, leading to a more uniform velocity profile across the fluid layer.

The variations in the temperature profile with Pr , Q , R and h_2 are shown in Figs. 10, 11, 12, and 13. The temperature profile decreases. As the Prandtl number increases, attributed to the ratio of thermal diffusivity to momentum diffusivity, the temperature profile decreases. Furthermore, the heat generation parameter inversely affects the temperature profile, while both the radiation parameter and thermal slip parameter directly impact it. Figures 14, 15, 16, and 17 show the changes in the concentration profiles for Sc , Kr , Sr and h_3 . Figure 14 shows how the concentration profile changes when Sc increases. A rise in Sc gives a decrease in molecular diffusivity, which leads to a decrease in concentration. This is due to the higher rate of diffusion of the solute in the fluid as

Fig. 4 Velocity profiles for different values of m

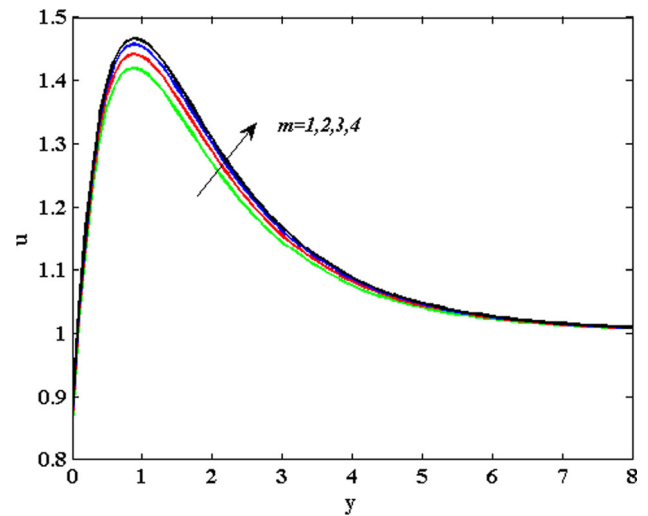


Fig. 5 Velocity profiles for different values of Gr

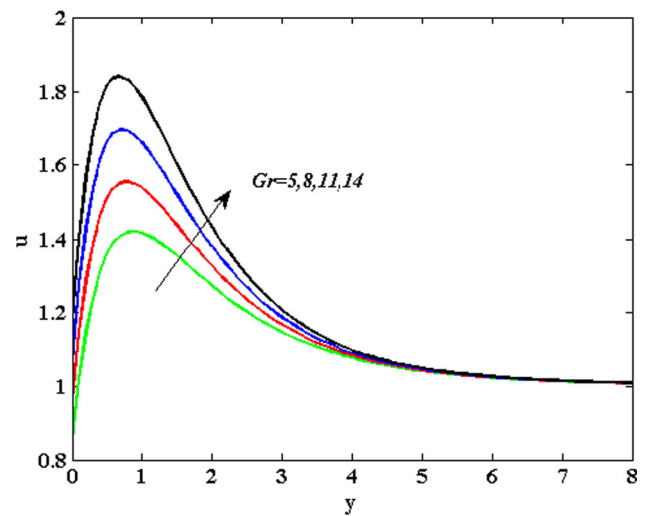
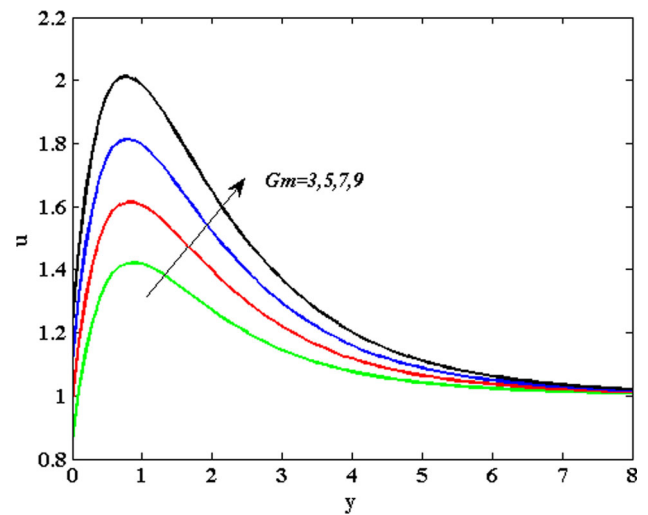


Fig. 6 Velocity profiles for different values of Gm



the Schmidt number increases. The concentration gradient increases, causing a faster decline in the concentration close to the plate. Figure 15 shows that the concentration profile decreases with increasing Kr. This phenomenon can be attributed to the enhanced mixing and dispersion of the fluid caused by the chemical reaction. A decrease in the concentration profile signifies a more efficient reaction process occurring at the surface of the plate. Figure 16 portrays the concentration profile for Sr. The concentration profile

Fig. 7 Velocity profiles for different values of λ

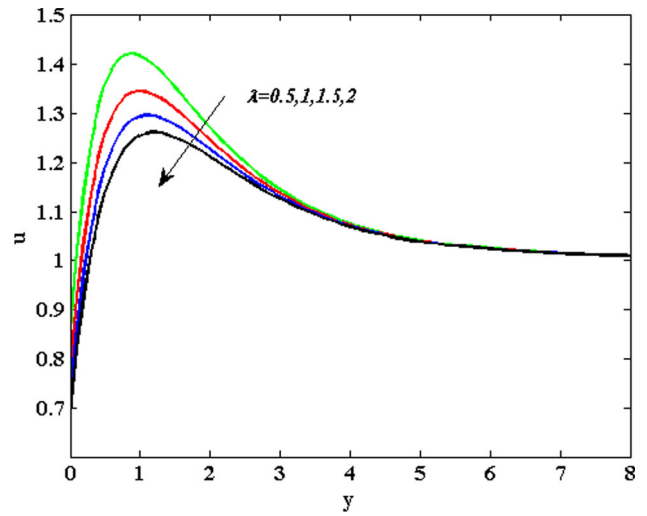


Fig. 8 Velocity profiles for different values of α

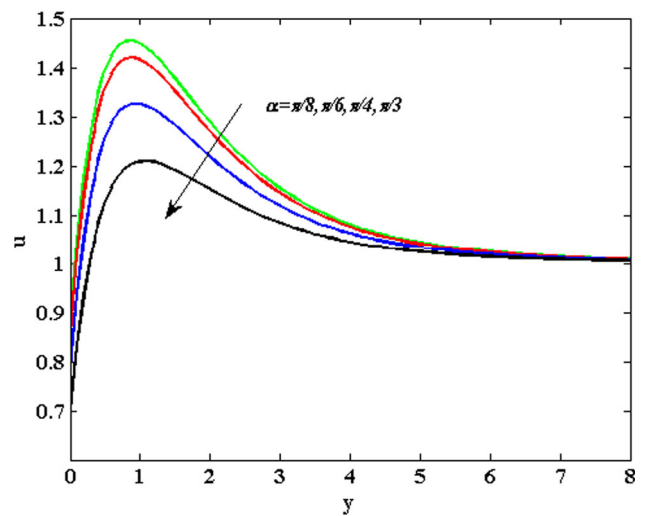
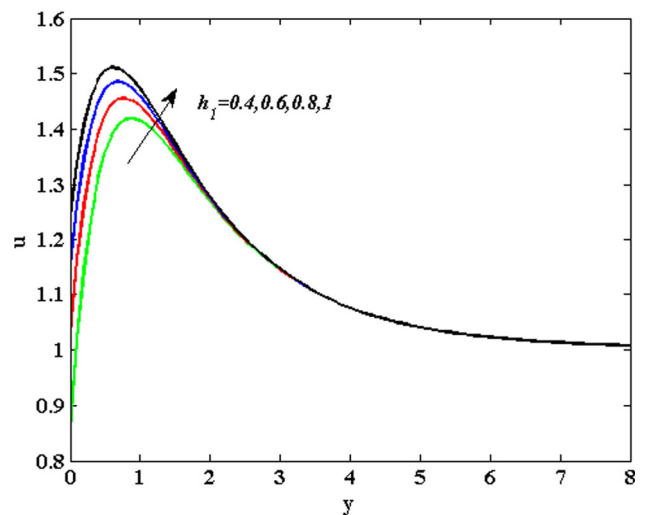


Fig. 9 Velocity profiles for different values of h_1



increases with increasing Sr . This phenomenon is a result of the thermal gradient causing the heavier fluid components to migrate toward the colder region, leading to a higher concentration near the plate. The Soret number quantifies the strength of this effect, with higher values indicating a more significant concentration profile. The concentration profile decreases with increasing h_3 , as shown in Fig. 17. A higher concentration slip parameter leads to greater mixing and dispersion of the fluid. As a result, the concentration

Fig. 10 Temperature profiles for different values of Pr

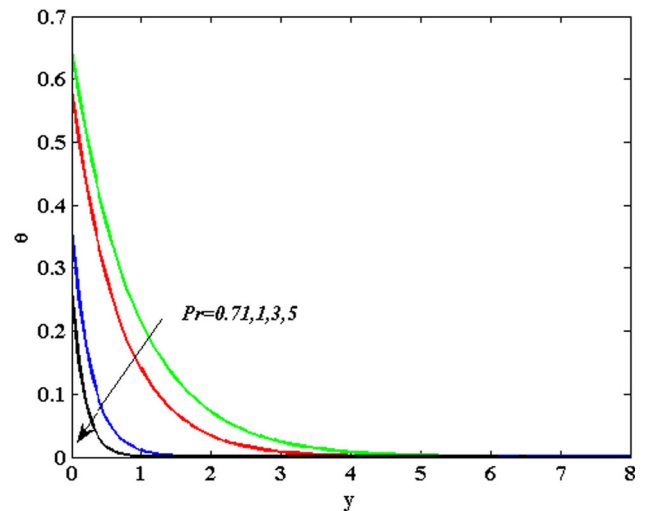
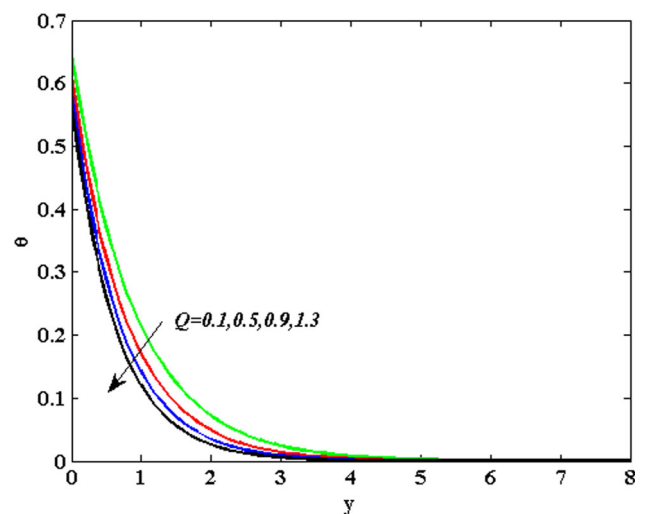


Fig. 11 Temperature profiles for different values of Q



gradient near the plate decreases more rapidly. Tables 1, 2, and 3 indicate the skin friction τ , Nusselt number Nu , and Sherwood number Sh . The skin friction coefficient decreases with increasing values of M , λ , and α , and the reverse trend is noted for the other parameters. This behavior is attributed to the fact that the magnetic field has a stabilizing effect on the flow of non-Newtonian fluids. Additionally, as the angle of inclination increases, the flow becomes more aligned with gravity, resulting in reduced skin friction. Since non-Newtonian fluids exhibit shear-thinning characteristics, the flow resistance decreases with increasing Jeffrey fluid parameter. The heat transfer rate increases with increasing values of Pr , Q , and R , while the opposite trend is detected for h_2 . This is because thermal slip reduces the thermal boundary layer thickness near the plate, leading to decreased heat transfer rates. Higher Prandtl numbers result in increased thermal boundary layer thickness, which enhances heat transfer. Additionally, the presence of a heat source and thermal radiation contribute to additional energy transfer mechanisms, further increasing the Nusselt number. This indicates that the convective heat transfer coefficient is influenced by these factors. The Sherwood number increases with increasing values of Sc and Kr and decreases with increasing values of Sr and h_3 . This indicates that the rate of mass transfer is influenced by both the diffusion of momentum and the chemical reaction occurring at the surface. To assess the robustness of our results, we conducted a comparative analysis with previous research investigations, as documented in Table 4, revealing a stronger alignment.

4 Conclusions

In this paper, we provide a novel and in-depth exploration of the behavior of Jeffrey fluids, shedding light on their pivotal roles in both biological systems and diverse industrial applications. Our investigation delved into the intricate dynamics of Jeffrey fluids under the influence of slip conditions, thermal effects, magnetic fields, and chemical interactions. This research is poised to revolutionize the field of drug delivery, offering the promise of more efficient and precise medication administration within the human body, thereby enhancing patient outcomes. Beyond the realm of medicine, the versatility of the Jeffrey fluid model has far-reaching implications

Fig. 12 Temperature profiles for different values of R

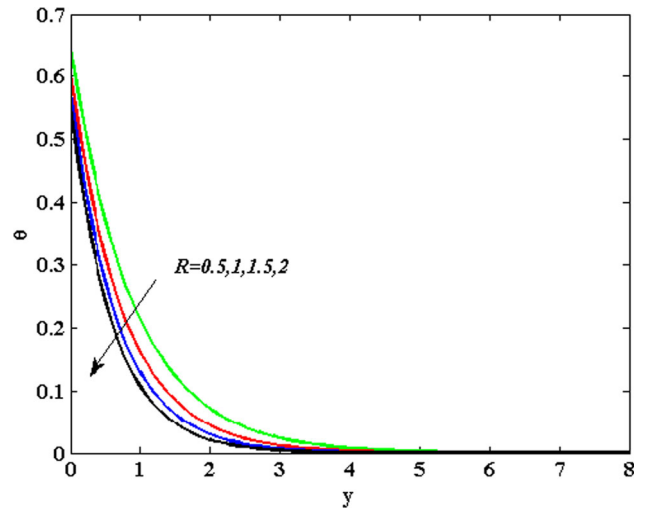


Fig. 13 Temperature profiles for different values of h_2

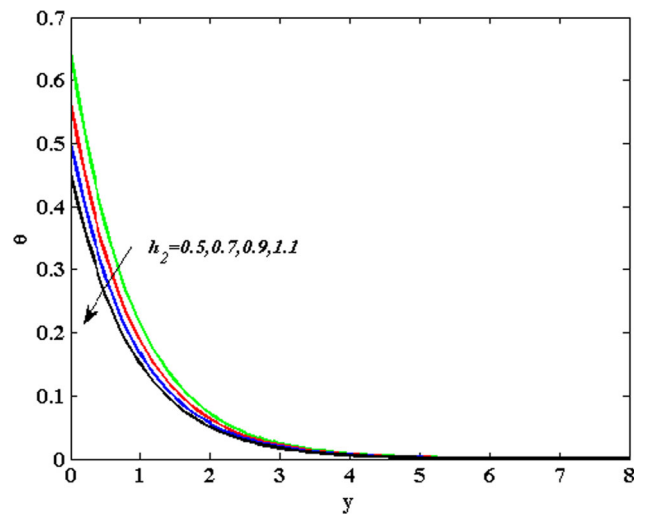
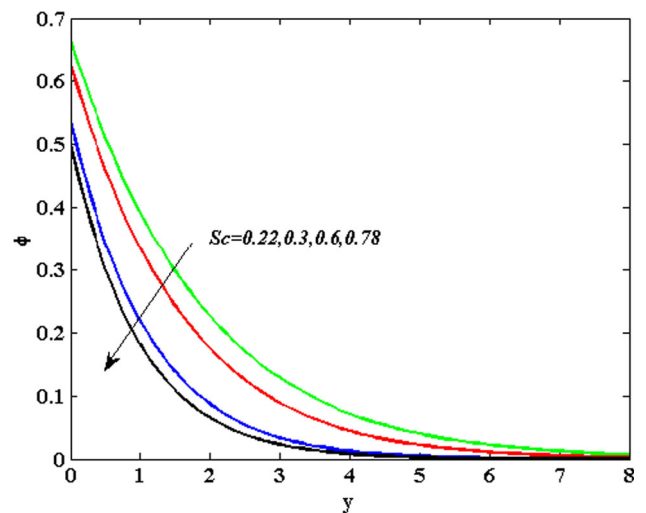


Fig. 14 Concentration profiles for different values of Sc



across various industrial sectors. Its applicability extends to domains such as foams, syrups, polymeric and metallurgical materials, as well as flow control mechanisms. Our analytical approach, rooted in the perturbation technique, provides a comprehensive understanding of mixed convective Jeffrey fluid flow over an inclined vertical plate. This analysis accounts for the intricate interplay

Fig. 15 Concentration profiles for different values of Kr

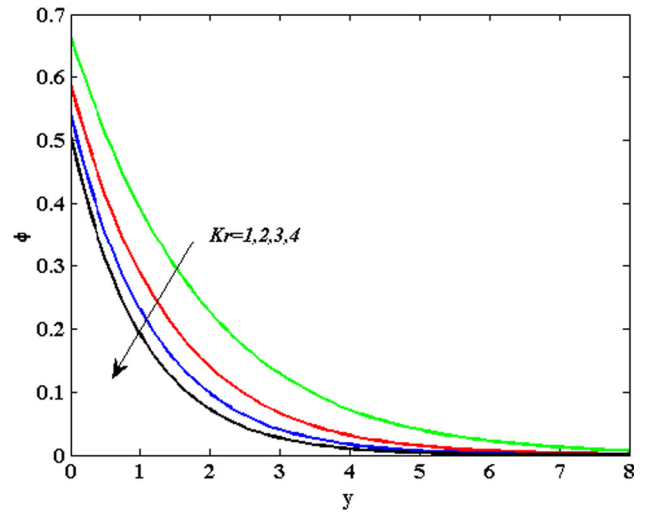


Fig. 16 Concentration profiles for different values of Sr

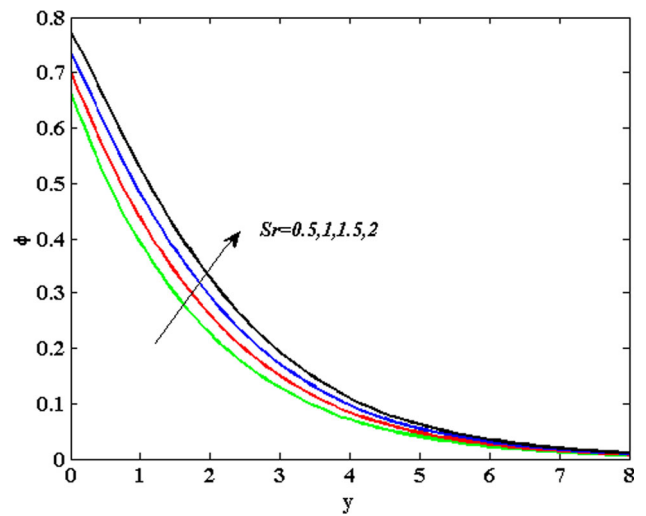
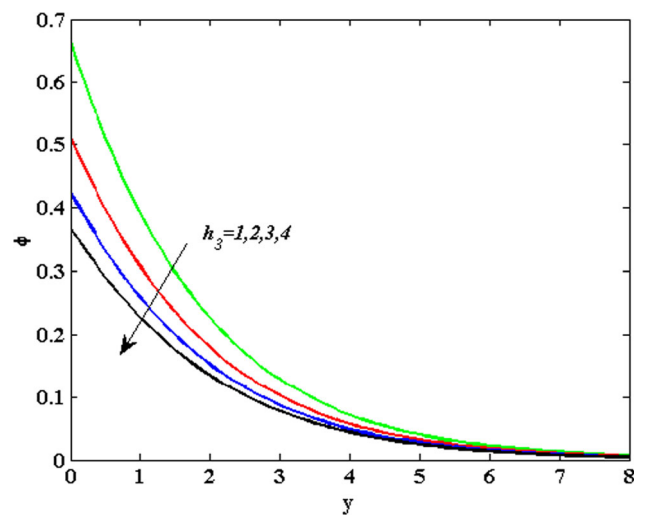


Fig. 17 Concentration profiles for different values of h_3



between the Soret and Hall currents, as well as slip conditions. Our research not only advances fundamental knowledge but also offers practical solutions for real-world challenges in fluid dynamics and material science.

The main findings of this study are as follows:

- As K , m , Gr and Gm increase, the velocity profiles increase. However, when λ and α are increased, the opposite effect occurs.

Table 1 Numerical values of the skin friction coefficient for various values of $M, K_p, m, Gr, Gm, \lambda$ and h_3

M	K_p	m	Gr	Gm	λ	h_3	α	γ	τ
1	0.5	0.5	5	3	0.5	0.4	$\pi/6$	$\pi/3$	1.8827
2	0.5	0.5	5	3	0.5	0.4	$\pi/6$	$\pi/3$	1.8399
3	0.5	0.5	5	3	0.5	0.4	$\pi/6$	$\pi/3$	1.8073
1	1	0.5	5	3	0.5	0.4	$\pi/6$	$\pi/3$	1.9890
1	1.5	0.5	5	3	0.5	0.4	$\pi/6$	$\pi/3$	2.0380
1	0.5	1	5	3	0.5	0.4	$\pi/6$	$\pi/3$	1.9022
1	0.5	1.5	5	3	0.5	0.4	$\pi/6$	$\pi/3$	1.9159
1	0.5	0.5	8	3	0.5	0.4	$\pi/6$	$\pi/3$	2.1486
1	0.5	0.5	11	3	0.5	0.4	$\pi/6$	$\pi/3$	2.4145
1	0.5	0.5	5	5	0.5	0.4	$\pi/6$	$\pi/3$	2.1919
1	0.5	0.5	5	7	0.5	0.4	$\pi/6$	$\pi/3$	2.5010
1	0.5	0.5	5	3	1	0.4	$\pi/6$	$\pi/3$	1.6893
1	0.5	0.5	5	3	1.5	0.4	$\pi/6$	$\pi/3$	1.5622
1	0.5	0.5	5	3	0.5	0.6	$\pi/6$	$\pi/3$	1.5477
1	0.5	0.5	5	3	0.5	0.8	$\pi/6$	$\pi/3$	1.3139
1	0.5	0.5	5	3	0.5	0.4	$\pi/4$	$\pi/3$	1.7163
1	0.5	0.5	5	3	0.5	0.4	$\pi/3$	$\pi/3$	1.4994
1	0.5	0.5	5	3	0.5	0.4	$\pi/6$	$\pi/6$	1.9189
1	0.5	0.5	5	3	0.5	0.4	$\pi/6$	$\pi/8$	1.9274

Table 2 Numerical values of the Nusselt number for various values of Pr, Q, R and h_2

Pr	Q	R	h_2	Nu
0.71	0.1	0.5	0.5	0.7092
1	0.1	0.5	0.5	0.8315
3	0.1	0.5	0.5	1.2749
0.71	0.5	0.5	0.5	0.7768
0.71	0.9	0.5	0.5	0.8284
0.71	0.1	1	0.5	0.7909
0.71	0.1	1.5	0.5	0.8503
0.71	0.1	0.5	0.7	0.6211
0.71	0.1	0.5	0.9	0.5524

Table 3 Numerical values of the Sherwood number for various values of Sc, Kr, Sr , and h_3

Sc	Kr	Sr	h_3	Sh
0.22	1	0.5	1	0.3352
0.3	1	0.5	1	0.3731
0.6	1	0.5	1	0.4635
0.22	2	0.5	1	0.4101
0.22	3	0.5	1	0.4573
0.22	1	1	1	0.2986
0.22	1	1.5	1	0.2620
0.22	1	0.5	2	0.2444
0.22	1	0.5	3	0.1923

- The temperature profile decreases as Pr, Q, R and h_2 increase.
- The concentration profile increases with increasing Sr concentration. However, the concentration profile diminishes with increasing Sc, Kr and h_3 .

This study serves as a foundation for future research endeavors aimed at harnessing the unique properties of Jeffrey fluids for advancements in both the scientific and industrial domains.

Table 4 Comparison of the Nusselt number values with those of Gulle et al. [25] when $A = 1$, $n = 0.1$, $t = 0.5$, and $\varepsilon = 0.2$

Pr	Q	Nu (Gulle et al. [25])	Present
0.71	1	- 15.796	- 1.5449
2	1	- 3.4690	- 3.3144
7	1	- 10.7271	- 9.5431
0.71	2	- 1.7797	- 1.8274
0.71	3	- 2.3370	- 2.0618

Data Availability We do not analyze or generate any datasets because our work proceeds within a theoretical and mathematical approach.

Appendix

$$m_1 = \frac{\text{Pr} + \sqrt{\text{Pr}^2 + 4 \text{Pr} \xi}}{2}$$

$$m_2 = \frac{\text{Pr} + \sqrt{\text{Pr}^2 + 4 \text{Pr}(\xi + \frac{n}{4})}}{2}$$

$$m_3 = \frac{\text{Sc} + \sqrt{\text{Sc}^2 + 4 \text{ScKr}}}{2}$$

$$m_4 = \frac{\text{Sc} + \sqrt{\text{Sc}^2 + 4 \text{Sc}(\text{Kr} + \frac{n}{4})}}{2}$$

$$m_5 = \frac{1 + \sqrt{1 + 4\lambda_1 N}}{2}$$

$$m_6 = \frac{1 + \sqrt{1 + 4\lambda_1(N + \frac{n}{4})}}{2}$$

$$A_1 = \frac{1}{1 + m_1 h_2}$$

$$A_2 = \frac{-A_3(1 + m_1 h_2)}{(1 + m_2 h_2)}$$

$$A_3 = \frac{\text{Pr} A m_1 A_1}{m_1^2 - \text{Pr} m_1 - \text{Pr}(\xi + \frac{n}{4})}$$

$$A_4 = \frac{1 - A_5(1 + m_1 h_3)}{1 + m_3 h_3}$$

$$A_5 = \frac{-\text{Sc} S r m_1^2 A_1}{m_1^2 - \text{Sc} m_1 - \text{ScKr}}$$

$$A_6 = \frac{-A_7(1 + h_3 m_3) - A_8(1 + h_3 m_2) - A_9(1 + h_3 m_1)}{(1 + h_3 m_4)}$$

$$A_7 = \frac{\text{Sc} A m_3 A_4}{m_3^2 - \text{Sc} m_3 - \text{Sc}(\text{Kr} + \frac{n}{4})}$$

$$A_8 = \frac{-\text{Sc} S r m_2^2 A_2}{m_2^2 - \text{Sc} m_2 - \text{Sc}(\text{Kr} + \frac{n}{4})}$$

$$A_9 = \frac{\text{Sc} m_1 (A A_5 - S r m_1 A_3)}{m_1^2 - \text{Sc} m_1 - \text{Sc}(K r + \frac{n}{4})}$$

$$A_{10} = \frac{u_w - A_{11}(1 + h_1 m_3) - A_{12}(1 + h_1 m_1) - 1}{(1 + h_1 m_5)}$$

$$A_{11} = \frac{-\text{Gm} A_4 \cos \alpha}{\lambda_1 m_3^2 - m_3 - N}$$

$$A_{12} = \frac{-(\text{Gr} A_1 \cos \alpha + \text{Gm} A_5 \cos \alpha)}{\lambda_1 m_1^2 - m_1 - N}$$

$$A_{13} = \frac{-A_{14}(1+h_1m_5) - A_{15}(1+h_1m_4) - A_{16}(1+h_1m_3) - A_{17}(1+h_1m_2) - A_{18}(1+h_1m_1) - 1}{(1+h_1m_6)}$$

$$A_{14} = \frac{Am_5A_{10}}{\lambda_1m_5^2 - m_5 - (N + \frac{n}{4})}$$

$$A_{15} = \frac{-GmA_6 \cos \alpha}{\lambda_1m_4^2 - m_4 - (N + \frac{n}{4})}$$

$$A_{16} = \frac{Am_3A_{11} - GmA_7 \cos \alpha}{\lambda_1m_3^2 - m_3 - (N + \frac{n}{4})}$$

$$A_{17} = \frac{-(GmA_8 \cos \alpha + GrA_2 \cos \alpha)}{\lambda_1m_2^2 - m_2 - (N + \frac{n}{4})}$$

$$A_{18} = \frac{(Am_1A_{12} - GrA_3 \cos \alpha - GmA_9 \cos \alpha)}{\lambda_1m_1^2 - m_1 - (N + \frac{n}{4})}$$

References

1. H. Alfvén, Existence of electromagnetic-hydrodynamic waves. *Nature* **150**(3805), 405–406 (1942)
2. G. Manjunatha, C. Rajashekhar, H. Vaidya, K.V. Prasad, O.D. Makinde, J.U. Viharika, Impact of variable transport properties and slip effects on MHD Jeffrey fluid flow through channel. *Arab. J. Sci. Eng.* **45**, 417–428 (2020)
3. B. HariBabu, P. Srinivasa Rao, S.V.K. Varma, Hall and ion-slip effects on MHD free convection flow of rotating Jeffrey fluid over an infinite vertical porous surface. *Heat Transf.* **50**(2), 1776–1798 (2021)
4. E.H. Hall, On a new action of the magnet on electric currents. *Am. J. Math.* **2**(3), 287–292 (1879)
5. M. Fiza, A. Alsubie, H. Ullah, N.N. Hamadneh, S. Islam, I. Khan, Three-dimensional rotating flow of MHD Jeffrey fluid flow between two parallel plates with impact of hall current. *Math. Probl. Eng.* **19**, 1–9 (2021)
6. H. Ullah, A. Alsubie, M. Fiza, N.N. Hamadneh, S. Islam, I. Khan, Impact of Hall current and nonlinear thermal radiation on Jeffrey nanofluid flow in rotating frame. *Math. Probl. Eng.* **2021**, 1–21 (2021)
7. M.V. Krishna, Hall and ion slip effects on radiative MHD rotating flow of Jeffreys fluid past an infinite vertical flat porous surface with ramped wall velocity and temperature. *Int. Commun. Heat Mass Transfer* **126**, 105399 (2021)
8. R.S. Raju, B.M. Reddy, G.J. Reddy, Finite element solutions of free convective Casson fluid flow past a vertically inclined plate submitted in magnetic field in presence of heat and mass transfer. *Int. J. Comput. Methods Eng. Sci. Mech.* **18**(4–5), 250–265 (2017)
9. K.V. Raju, A. Parandhama, M.C. Raju, K.R. Babu, Unsteady MHD mixed convection flow of Jeffrey fluid past a radiating inclined permeable moving plate in presence of thermophoresis heat generation and chemical reaction. *J. Ultra Sci. Phys. Sci.* **30**(1), 51–65 (2018)
10. L. Manjula, R. Muthucumaraswamy, Heat and mass transfer effect on an infinite vertical plate in the presence of hall current and thermal radiation with variable temperature. *Int. J. Appl. Mech. Eng.* **26**(3), 131–140 (2021)
11. N. Kanimozhi, R. Vijayaragavan, K. Shanmugam, Impacts of thermal radiation, viscous dissipation, ohmic heating, and diffusion-thermo effects on unsteady MHD free convective rotating flow of second-grade fluid with Hall and ion-slip currents. *Heat Transf.* **51**(8), 7435–7461 (2022)
12. M. Qasim, Heat and mass transfer in a Jeffrey fluid over a stretching sheet with heat source/sink. *Alex. Eng. J.* **52**, 571–575 (2013)
13. T. Hayat, S.A. Shehzad, M. Qasim, S. Obaidat, Radiative flow of a Jeffrey fluid in a porous medium with power law heat flux and heat source. *Nucl. Eng. Des.* **243**, 15–19 (2012)
14. M. Kothandapani, S. Srinivas, Peristaltic transport of a Jeffrey fluid under the effect of magnetic field in an asymmetric channel. *Int. J. Nonlinear Mech.* **43**(9), 15–24 (2008)
15. S. Nadeem, N.S. Akbar, Peristaltic flow of a Jeffrey fluid with variable viscosity in an asymmetric channel. *Z. für Naturforschung A* **64**(11), 713–722 (2009)
16. R. Ellahi, M.M. Bhatti, I. Pop, Effects of hall and ion slip on MHD Peristaltic flow of Jeffrey fluid in a nonuniform rectangular duct. *Int. J. Numer. Meth. Heat Fluid Flow* **26**(6), 1802–1820 (2016)
17. K. Ramesh, D. Tripathi, O.A. Beg, A. Kadir, Slip and hall current effects on Jeffrey fluid suspension flow in a peristaltic hydromagnetic blood micropump. *Iran. J. Sci. Technol. Trans. Mech. Eng.* **43**, 675–692 (2019)
18. K.R. Babu, A. Parandhama, K.V. Raju et al., Unsteady MHD free convective flow of a visco-elastic fluid past an infinite vertical porous moving plate with variable temperature and concentration. *Int. J. Appl. Comput. Math* **3**, 3411–3431 (2017)
19. M.T. Sk, K. Das, P.K. Kundu, Multiple slip effects on bioconvection of nanofluid flow containing gyrotactic microorganisms and nanoparticles. *J. Mol. Liq.* **220**, 518–526 (2016)
20. N. Kanimozhi, R. Vijayaragavan, S. Karthikeyan, Multiple slip impacts on unsteady MHD micropolar fluid past a stretching sheet with non-Darcy porous medium and uneven heat source/sink. *Heat Transf.* **52**(7), 4732–4754 (2023)
21. K.S. Balamurugan, J.L. Ramaprasad, S.V.K. Varma, Unsteady MHD free convective flow past a moving vertical plate with time dependent suction and chemical reaction in a slip flow regime. *Procedia Eng.* **127**, 516–523 (2015)
22. P.S. Narayana, D.H. Babu, Numerical study of MHD heat and mass transfer of a Jeffrey fluid over a stretching sheet with chemical reaction and thermal radiation. *J. Taiwan Inst. Chem. Eng.* **59**, 18–25 (2016)
23. K. Das, N. Acharya, P.K. Kundu, Radiative flow of MHD Jeffrey fluid past a stretching sheet with surface slip and melting heat transfer. *Alex. Eng. J.* **54**(4), 815–821 (2015)
24. P.P. Kumar, B.S. Goud, B.S. Malga, Finite element study of Soret number effects on MHD flow of Jeffrey fluid through a vertical permeable moving plate. *Partial Differ. Equ. Appl. Math.* **1**, 100005 (2020)
25. N. Gulle, R. Kodi, Soret radiation and chemical reaction effect on MHD Jeffrey fluid flow past an inclined vertical plate embedded in porous medium. *Mater. Today Proc.* **50**, 2218–2226 (2022)
26. M.A. Kumar, Y.D. Reddy, B.S. Goud, V.S. Rao, Effects of soret, dufour, hall current and rotation on MHD natural convective heat and mass transfer flow past an accelerated vertical plate through a porous medium. *Int. J. Thermofluids* **9**, 100061 (2021)

27. K.S. Nisar, R. Mohapatra, S.R. Mishra, M.G. Reddy, Semianalytical solution of MHD free convective Jeffrey fluid flow in the presence of heat source and chemical reaction. *Ain Shams Eng. J.* **12**(1), 837–845 (2021)
28. S. Saleem, M. Abd El-Aziz, Entropy generation and convective heat transfer of radiated non-Newtonian power-law fluid past an exponentially moving surface under slip effects. *Eur. Phys. J. Plus* **134**(4), 184 (2019)
29. N.A. MohdZin, I. Khan, S. Shafie, Exact and numerical solutions for unsteady heat and mass transfer problem of Jeffrey fluid with MHD and Newtonian heating effects. *Neural Comput. Appl.* **30**(11), 3491–3507 (2018)
30. M. Abd El-Aziz, A.S. Yahya, Perturbation analysis of unsteady boundary layer slip flow and heat transfer of Casson fluid past a vertical permeable plate with Hall current. *Appl. Math. Comput.* **307**, 146–164 (2017)
31. T. Hayat, M.B. Ashraf, H.H. Alsulami, On mixed convection flow of Jeffrey fluid over an inclined stretching surface with thermal radiation. *Heat Transf. Res.* **46**(6), 515–539 (2015)
32. T. Hayat, A. Shafiq, A. Alsaedi, M. Awais, MHD axisymmetric flow of third grade fluid between stretching sheets with heat transfer. *Comput. Fluids* **86**, 103–108 (2013)
33. N.A.M. Noor, S. Shafie, M.A. Admon, Unsteady MHD squeezing flow of Jeffrey fluid in a porous medium with thermal radiation, heat generation/absorption and chemical reaction. *Phys. Scr.* **95**(10), 105213 (2020)
34. O.D. Makinde, I.L. Animasaun, Bioconvection in MHD nanofluid flow with nonlinear thermal radiation and quartic autocatalysis chemical reaction past an upper surface of a paraboloid of revolution. *Int. J. Therm. Sci.* **109**, 159–171 (2016)
35. D. Srinivasacharya, K.H. Bindu, Entropy generation of micropolar fluid flow in an inclined porous pipe with convective boundary conditions. *Sādhanā* **42**, 729–740 (2017)
36. J. Prakash, A. Sharma, D. Tripathi, Thermal radiation effects on electroosmosis modulated peristaltic transport of ionic nanoliquids in biomicrofluidics channel. *J. Mol. Liq.* **249**, 843–855 (2018)
37. P. Rana, M.J. Uddin, Y. Gupta, A.M. Ismail, Slip effects on MHD Hiemenz stagnation point nanofluid flow and heat transfer along a nonlinearly shrinking sheet with induced magnetic field: multiple solutions. *J. Braz. Soc. Mech. Sci. Eng.* **39**, 3363–3374 (2017)
38. M.G. Ibrahim, M.Y. Abou-Zeid, Computational simulation for MHD peristaltic transport of Jeffrey fluid with density-dependent parameters. *Sci. Rep.* **13**(1), 9191 (2023)
39. J. Dong, D. Li, M. Yu, K. Li, Research on electromagnetic electroosmotic flow of Jeffrey fluid through semicircular microchannel. *Eng. Res. Express* **5**(4), 045083 (2023)
40. D. Thenmozhi, M.E. Rao, R.R. Devi, C. Nagalakshmi, Analysis of Jeffrey fluid on MHD flow with stretching–porous sheets of heat transfer system. *Forces in Mech.* **11**, 100180 (2023)
41. D. Li, K. Li, H. Li, Pulse electromagnetic flow of Jeffrey fluid in parallel plate microchannels. *Phys. Scr.* **98**, 115202 (2023)
42. A. Khan, T. Gul, I. Ali, H.A. Khalifa, T. Muhammad, W. Alghamdi, A.A. Shaaban, Thermal examination for double diffusive MHD Jeffrey fluid flow through the space of disc and cone apparatus subject to impact of multiple rotations. *Int. J. Heat Fluid Flow* **106**, 109295 (2024)

Springer Nature or its licensor (e.g. a society or other partner) holds exclusive rights to this article under a publishing agreement with the author(s) or other rightsholder(s); author self-archiving of the accepted manuscript version of this article is solely governed by the terms of such publishing agreement and applicable law.